An Ab Initio Screening Approach for the Discovery of Lignin Polymer Breaking Pathways

Brendan D. Mar[1], Helena W. Qi[1,2], Fang Liu[3], and Heather J. Kulik[1,*]

[1]*Department of Chemical Engineering, Massachusetts Institute of Technology, Cambridge, Massachusetts, 02139 United States*

[2]*Department of Chemistry, Massachusetts Institute of Technology, Cambridge, Massachusetts, 02139 United States*

[2]*Department of Chemistry, Stanford University, Stanford, CA, 94305 United States*

Keywords: Density functional theory, steered molecular dynamics, biomass, lignocellulose, lignin.

The directed depolymerization of lignin biopolymers is of utmost relevance for the valorization, i.e. commercialization, of biomass fuels. We present a computational and theoretical screening approach to identify potential cleavage pathways and resulting fragments that are formed during depolymerization of lignin oligomers containing two to six monomers. We have developed a chemical discovery technique to identify the chemically relevant putative fragments in eight known polymeric linkage types of lignin. Obtaining these structures is a crucial precursor to the development of any further kinetic modeling. We have developed this approach by adapting steered molecular dynamics calculations under constant force and varying the points of applied force in the molecule to diversify the screening approach. Key observations include relationships between abundance and breaking frequency, the relative diversity of potential pathways for a given linkage, and the observation that readily-cleaved bonds can destabilize adjacent bonds, causing subsequent automatic cleavage.

1. Introduction

As the demand for finding and utilizing cheap and renewable energy sources mounts[1], more complex and heterogeneous feedstocks, such as biomass[2-3], are increasingly being considered. The valorization, or commercialization of a pathway to fuel from natural resources, of lignocellulosic biomass has captured much interest in recent years[4-7]. Lignin, in particular, is a structurally complex biopolymer[8], which currently is commercially utilized only for the fast pyrolysis[9-10] generation of low-grade bio oil[3] that is volatile and has been demonstrated to be of moderate utility[11]. The experimental catalysis community has been fascinated by the prospect of upgrading, or making more useful, lignin-derived bio oils through the catalytic removal of oxygen groups in a process known as hydrodeoxygenation or other more advanced catalytic routes, including using metabolic engineering[4, 12-14].

Nevertheless, the pyrolysis step to generate bio oil requires high temperatures and energy inputs and the bio oil product is not particularly stable for transportation. For that reason, understanding the structure of the unprocessed lignin polymer remains of interest[8, 15]. Recent experimental achievements have included depolymerization via polyoxometalate catalysts[16], base-catalyzed hydrolysis[17-18], acidolysis[19-20], ionic liquid treatment[21], reduction with hydrosilanes[22], photochemical degradation[23], and ball milling[24]. In addition to general depolymerization, efforts have also included selective strategies via homogeneous catalysts[25-29] and enzymes[30]. A route to selective depolymerization that both prevents repolymerization and generates a specific set of monomers[31] has only recently had success experimentally with the aid of metal catalysts[32-33] capable of producing up to 50% yield.

The natural structural complexity of the lignin biopolymer, which contains as many as eight known linkages between three monomeric units[16], is critical to understanding how to design a catalyst for selective depolymerization. This complexity may at first be daunting for first-principles, computational approaches due to the size of even minimal oligomers and their complex chemistry. Nevertheless, the complexity in polymeric feedstocks also mandates computational screening to identify the difference in local bonding environments in these complex molecules. In this work, we turn the problem of heterogeneous feedstocks on its head, proposing instead that substrate variability presents a rich selection of chemical bonds for study

and for future efforts as targets for computational and experimental design of selective catalysts, even as catalytic upgrading of bio oil continues to have successes in "making money" out of lignin, a notoriously intractable material. Lignin is noteworthy because it makes up roughly 20-30% by weight[34] of biomass. The key features of lignin as opposed to other components of biomass are that it is a heavily cross-linked polymer consisting of large numbers of phenolic moieties, making it the most abundant source of aromatic carbon in nature[16]. Lignin polymers are derived from p-coumaryl, sinapyl, and coniferyl alcohol monomers[16] that differ by the presence (sinapyl, coniferyl) or absence (p-coumaryl) of methoxy groups functionalizing the aromatic ring common to each monomer (see Fig. 3 later in the text). The coniferyl alcohol monomer makes up 90% of all softwood lignins[16], which also have some of the highest concentrations of lignin, and contains a single methoxy group.

A great deal of computational effort has been dedicated to studying model compounds that encapsulate some of the key linkages in lignin. Major focuses have been on identifying homolytic bond dissociation energies[35-36] and mechanical properties[37-40], intramolecular hydrogen bonding[41], kinetic modeling[42-43], and the effect of ionic liquids[44-45]. The most prolific and thorough researchers in this area have been Beste and Buchanan, who have carried out a number of studies on both phenethyl phenyl-ether (PPE) and its methoxy form to understand free energy pathways for homolytic bond cleavage events for C-C bonds and C-O bonds that occur during pyrolysis using B3LYP[46] and M06-2X functionals[47]. They followed up their initial work with further studies of bond dissociation enthalpies for additional substituted β-O-4 model compounds[48], kinetic analysis[42-43] including of phenyl-shift reactions with substituents on the phenyl ring vs. the phenyl ether[42] and hydrogen abstraction[49]. More recently, Beste has studied selectivity for pyrolysis products in PPE and α-hydroxy-PPE[50] and used reactive force fields to identify activation energy for conversions of dilignol model compounds[51]. However, it is worth noting that few, if any, computational studies have been carried out on larger models of lignin. Only limited, combined experimental and theoretical studies[52] have focused on the more complex chemistry of less abundant linkages. The more uniform cellulose has been very faithfully mechanistically and kinetically modeled computationally with relatively small model compounds[53], but such an approach would not be possible on the more heterogeneous lignin.

Inspired in part by recent experimental and computational efforts in efficient mechanistic study of mechanochemical depolymerization[54-60], we develop an alternative approach in which we employ steered molecular dynamics under constant force to understand lignin compound depolymerization. We focus here on models of lignin polymers comprised of coniferyl alcohol, the predominant monomer in softwood lignins. Our approach may be used to directly understand the effects of approaches that mechanically depolymerize lignin, such as ball milling[24], but, more importantly, we employ it here as a screening technique to identify the weakest bonds in lignin models and to follow the dynamical processes that occur when these bonds are broken. Such direct observations are not possible in homolytic bond dissociation energy studies. We also study the pathways for bond-breaking, not making any assumptions about bond-breaking mechanisms and, in select cases, identify the distances at which recombination is most favorable.

Following review of our screening methodology, we will present outcomes tested on lignin model systems. For these applications, we first present bond fragmentation patterns in small dimeric compounds, comparable to those studied previously in the literature. Next, we expand our studies to long, hexameric repeats that now include some of the polymeric character of lignin fragments. Hexameric models represent the largest model compounds studied from first-principles to date, although reactive force fields have been previously used on hexamers[61]. We study the effect that the presence of acid or base model catalysts has on bond-breaking pathways and the associated threshold at which bond cleavage occurs. Importantly, we observe unusual chemistries in branching models; namely 1) in a model of the recently discovered[62-63] spirodienone lignin linkage we observe over 23 unique pathways that result from our screen, and 2) we observe that cleavage of ether bonds in the dibenzodioxocin linkage can destabilize the more intractable remaining biphenyl linkage, leading to spontaneous C-C bond cleavage.

2. Screening Approach

Here, we introduce a screening approach for identification of fragmentation patterns in lignin model compounds. We employ an *ab initio* steered molecular dynamics approach that permits direct dynamics on the force-modified potential energy surface (FMPES). While this method has been previously demonstrated to be useful for mechanochemistry[54-60], we are instead developing this approach as a screening method. In any constant force dynamics method, an

attachment point (AP) is defined on the molecule that corresponds to an atom that is pulled at constant force to a pulling point (PP) that is a fixed point some distance away (examples of APs and AP-PP directions shown in Fig. 1). This external force is thus defined as:

$$\mathbf{F}_{ext} = \sum_{i}^{AP} F_i \frac{\mathbf{r}_i^{PP} - \mathbf{r}_i^{AP}}{\left\| \mathbf{r}_i^{PP} - \mathbf{r}_i^{AP} \right\|} \ , \tag{0}$$

where $\mathbf{r}_i^{AP/PP}$ is the position of the AP or PP and F_i are the applied force values. The total force in this approach is then a sum of the standard force from an *ab initio* evaluation of the gradient in addition to the applied external (ext) force:

$$\mathbf{F}_{total} = \mathbf{F}_{ab\ initio} + \mathbf{F}_{ext} \ . \tag{0}$$

Using this established approach, we recently reported[59] the mechanochemically-induced depolymerization of a low-ceiling temperature polymer poly-o-phthalaldehyde. There, we observed that a heterolytic bond-breaking mechanism led to propagation of further depolymerization events, thus "unzipping" the polymer. This preliminary success inspired our current development of force-modified molecular dynamics in order to identify whether any conditions would permit the unzipping of lignin polymer to monomers (flowchart overview in Fig. 2). This *ab initio* molecular dynamics approach permits direct identification of what the most readily cleaved bonds are in a molecule. We run molecular dynamics simulations at 300 K, and in this study we apply forces in the range of 1.0-4.0 nN to accelerate cleavage of the lowest-energy chemical bonds. A force of around 3.0 nN is anecdotally comparable to the level of forces achieved in a typical sonication experiment[54]. Even for a relatively high force of 4.0 nN, structures do not become substantially distorted: an equilibrium C-C bond distance in an aromatic ring of 1.42 Å will sample bond distances in the range of 1.37-1.48 Å, commensurate with those sampled during other types of accelerated molecular dynamics (see Supporting Information). Therefore, while we are using force to ensure bond breaking, we are unlikely to be dramatically altering the geometric structure from geometries preferred on the force-unmodified potential energy surface. Once a bond is cleaved, the simulation runs until the fragments reach the pulling points and the simulation is terminated.

Additional tunable parameters include, as with any electronic structure approach, the electronic structure method and the basis set employed. Here, we employ the long-range-corrected hybrid functional LRC-ωPBEh[64] with a modest 6-31g basis set. While outside the scope of this work, it may be advantageous in this screening approach to direct the electronic structure method and basis set choice to one that is known to underestimate or overestimate certain bond dissociation energies. All electronic structure methods will introduce some bias, be it overestimation of barrier heights in Hartree-Fock and high exact-exchange ratio hybrid functionals or underestimation in pure density functionals. This bias may then be directed towards enhancing sampling in the screening approach with subsequent energetic refinement at higher levels of theory. One may also accelerate such studies by choosing smaller basis sets, as was also used in the recently introduced "nanoreactor" for chemical discovery of bond-formation reactions[65]. There, reactions were dynamically discovered with a very minimal Hartree-Fock theory and 3-21g basis set combination, later followed-up by more detailed path-based transition-state search with hybrid exchange-correlation functionals and larger, polarized basis sets.

Activation energies and transition states are outside the scope of this preliminary work, where we instead emphasize the scale of electronic structure calculations and dynamics that may be surveyed. Here, we have studied up to six monomeric units (hexamers) of the most common linkage in lignin both its standard form and in the presence of a catalyst. We also present extensive dimer and trimer models of all eight linkages in lignin. We harness recent advances in stream processing hardware and algorithmic developments[66-68] that have been demonstrated to be successful in proteins[69-71] to accelerate this biopolymer-oriented screening approach. For those unfamiliar with TeraChem[72] or typical GPU performance, our ωPBEh/6-31g calculations require 10-30s/timestep on 2 GPUs for the dimer model and 60-110s on 2-4 GPUs for the hexamer.

In order to give a sense of the scale of the screening effort, our dimer and trimer studies were carried out on 8 different linkages with a variety of attachment points, i.e. atoms on the molecules to which the force is directly applied (see Fig. 1). Two gas-phase trajectories were run for each unique pair of attachment points, producing 50 4.0 nN trajectories that were each at least 1.25 ps in length. This runtime corresponds to each calculation on a dimer taking about a day for a 0.25 fs timestep. The pulling points were placed 15 Å from the attachment points on the dimer.

A 4.0 nN force was chosen because it is on the higher side of experimentally reproducible forces in sonication experiments[55-56, 59] and was likely to produce at least some bond-breaking events for the majority of linkages. Due to the high value of the applied force, attachment points were limited to sites on the rings of the lignin monomers, rather than terminal carbons.

In the case of hexamers, we constructed these molecules from six repeats of coniferyl alcohol connected via five β-O-4 linkages with the same stereochemistry as the dimers (see Fig. 3). Our screening approach on the hexamer model compounds features an examination of the force dependence as a proxy for identifying the efficacy of a model catalyst. We consider lower forces, which range from 1.0 to 3.5 nN, on the hexameric compound based on previous observations that lower forces are needed in larger molecules, likely due to compensating delocalization of electron density over larger fragments. Pulling points are placed 25 Å from the attachment points (methoxy carbons) on the hexameric compounds, in order to compensate for the longer length of the molecule. Since larger molecules are more susceptible to breaking at lower forces and require longer distances between AP and PP to ensure that the fragmentation does not lead to pulling the APs to the PPs too quickly at higher force. Once the AP reaches the PP, there is no longer a force felt on the system and this could lead to disruption of the observation of dynamic rearrangements. We emphasize here that the primary focus of this screening effort is to ensure the discovery of dynamic rearrangement following bond cleavage that is not as accessible in more commonly employed homolytic bond dissociation energy studies.

Under the aforementioned constraints, we also introduce model catalysts and identify how their presence alters the force-dependent profile of cleavage events. Here we use hydronium ion to model acid catalysis and tertbutoxide anion to model base catalysis. We place the species in the simulation and position them one at a time near each of the five linkages. In order to ensure sufficient statistics, we run five trajectories for each catalyst at each position for 2-3 ps for a total of 25 trajectories at each force value. These studies permit the determination of whether any cleavage events differ strongly in the presence of a model catalyst. In order to carry out catalyst-design-based screens, one would more likely use model reaction mechanisms obtained during this initial screen and then carry out minimum-energy path search techniques. This subsequent screen would then focus on the known rate-determining step(s) using a most

abundant reactive intermediate – least stable transition state approach[73-75] to maximize kinetic turnover. However, the current study focuses on identification and prediction of model compounds, paving the way for future study that will enable catalyst screening. Our screening also likely identifies fragments that could form during experiments carried out under extreme environments such as pyrolysis or ball milling.

3. Computational Methods

We employ the TeraChem code to carry out ab initio steered molecular dynamics (AISMD) calculations[55]. By using an applied constant force in the range of 1.5 nN to 4.0 nN, we carry out dynamics directly on the force-modified potential energy surface (FMPES), as has been previously demonstrated, e.g. in Refs. [55, 57]. The AISMD simulations were carried out with unrestricted density functional theory (DFT) using the long-range-corrected, ωPBEh exchange-correlation functional (ω=0.2)[76] and the 6-31g basis set. All AISMD simulations were carried out with a 0.25 fs timestep. In order to encourage convergence, where favorable, to an unrestricted, radical solution, level-shifting (a 1.0 eV shift was applied to α states, 0.0 eV on β states)[77]. Hexameric acid and base catalysis studies were repeated with an accelerated implementation[78] of the conductor-like implicit solvation model (COSMO)[78-80] using a dielectric of ε=80, but there was no observed change to bond-breaking events. For cases where a variable force screening was completed, such as in the hexamer, once a force threshold was reached where 100% breaking was observed, only five trajectories were also completed at higher thresholds (e.g. 3.0 nN and 3.5 nN for the acid and the base) to verify complete breaking occurred at these force thresholds. For each trajectory, natural bond orbitals (NBO) were obtained using the NBO6[81] interface to TeraChem. The NBO analysis categorizes transformed orbitals as core, two-center or three-center bonding orbitals, and lone pairs for the generation of Lewis structures. This analysis also categorizes the extent of electron density that is non-Lewis in nature. The occupancy of each Lewis-like lone pair NBO may be assessed, with distinct spin up and down orbitals centered around the cleaved bond corresponding to radical, homolytic cleavage.

4. Results and Discussion

4a. Dimer studies

An ongoing goal for lignin utilization is to effectively decompose the complex polymer into useful valuable chemicals. When bonds in lignin are cleaved, a large variety of products may be formed, and the variability in products of pyrolysis or other depolymerization processes leaves lignin the most underutilized component of biomass[82]. One select linkage, the β-O-4 ether (C-O-C) linkage, represents around 50% of the lignin monomer linkages in most woods, while the other types of linkages including 5-5' biphenyl linkage (aromatic C-C), β-5, and 4-O-5 diaryl ether represent no more than 25% individually of the remaining linkages (see structures in Fig. 3 and abundance in Fig. 4)[34].

For preliminary studies of dimers and trimers, we assembled coniferyl alcohol monomers to produce the eight most common linkages in softwood lignin: β-O-4 (abundance, *ab*=46%), 5-5 (*ab*=23.5%), β-5 (*ab*=10%), dibenzodioxocin (*ab*=6.5%), 4-O-5 (*ab*=5.5%), β-β (*ab*=3.5%), β-1 (*ab*=3%), and spirodienone (*ab*=2%)[16] (see also abundances in Fig. 4). Dimer studies provided a preliminary screen to identify which linkages were most amenable to mechanochemical bond-breaking for subsequent larger-scale simulations. For each dimeric linkage, we carried out 50 4.0 nN steered MD simulations (1-4 ps in length) and report the percentage of simulations that lead to bond cleavage alongside the abundance in softwood lignin (see Fig. 4) and range of times at which bond cleavage occurs (see Supporting Information). We note that cleavage frequency corresponds to the likelihood of observation of a breaking event at our constant 4.0 nN, bond dissociation energies (see Supporting Information) are likely more comparable with force-dependent cleavage profiles, as we carry out later in this work when evaluating model acid/base catalysts (see Sec. 4d). We also discuss how attachment point choices influence cleavage frequency in more detail in Sec. 4c. Dibenzodioxocin and spirodienone linkages are minimally-defined by three monomers, and an even larger number of simulations, 112 and 150, respectively were carried out on these trimers. Stereochemistry, where applicable, is indicated in Fig. 3 for each compound. Bond cleavage primarily occurs early on in these simulations (~250-500fs), but dynamics are continued for at least around 3 ps to capture rearrangement and relaxation after cleavage. The relatively rapid observation of cleavage events motivates this force-based screening approach (requiring only ~1000-10,000 gradient evaluations) as a screening technique to identify bond fragmentation because such events would take nearly infinite timescales in direct Born-Oppenheimer molecular dynamics at moderate temperatures. Conversely, path-based

searching techniques would require *a priori* knowledge of the reactant and product endpoints involved in fragmentation. There are a few notable exceptions to the rapid cleavage timescales. Some slower bond-cleavage (~2 ps) was observed for β-O-4 linkages, and these late cleavage events suggest that the percentage of bond cleavage events might increase if dynamics were continued for longer timeframes (see Supporting Information). When cleavage occurred on longer timescales for other linkages (e.g. spirodienone), this delay was primarily the result of sequential bond-cleavage events.

The predominance of both β-O-4 and 5-5 linkages in softwood lignin make them of primary interest for any computational lignin study. However, we observed no bond-breaking events for 5-5 linkages, due to the fact that cleavage of this biphenyl-like C-C linkage necessitates disruption of the aromaticity of both of the monomers' phenolic rings. Inclusion of specific model catalysts capable of cleaving C-C bonds would likely be necessary to facilitate 5-5 cleavage during these steered MD simulations, but we will revisit 5-5-like cleavage shortly in the context of dibenzodioxocin trimeric branching linkages (see Sec. 4b). The less abundant (*ab*=5.5%) 4-O-5 linkage also has a relatively low cleavage frequency (*cf*=4%). In this case, the phenyl groups of neighboring monomers are linked through an ether bond, and the rarely observed (C-O) cleavage events occur through formation of a benzene radical fragment, which is subsequently stabilized through hydrogen transfer (see Supporting Information).

In contrast to 5-5 linkages (*cf*=0%), the β-O-4 linkage breaks frequently in our simulations (*cf*=56%). Two primary pathways were observed for the cleavage of β-O-4 linkages: one involved simple homolytic bond cleavage of the C(β)-O bond and separation to radical fragments, while the other involved homolytic bond cleavage followed by hydrogen transfer leading to closed shell fragments (Fig. 5). In the former case, this mechanism is identical that has been proposed before for β-O-4 homolytic bond cleavage (e.g. see Fig. 4g in Ref. [51]), thus validating that we are not substantially diverging from previous computational studies through incorporation of a steering force. In the second case, the transferred hydrogen atom originated either from a neighboring alcohol group or directly from the adjacent carbon atom, leading to either aldehyde or enol products (for a total of three overall pathways). We selected snapshots of monomers after cleavage at various separation distances to identify whether fragments would recombine or rearrange once the constant force was turned off. Recombination did not occur for

separation distances greater than 2.3 Å, but hydrogen transfer continued for distances up to 5 Å. These recombination studies suggest a predominant mechanism of homolytic bond cleavage to form radicals followed by hydrogen atom transfer to produce closed shell fragments.

A number of homolytic bond dissociation energy studies[35-36, 47-48] have been carried out on models, particularly of the β-O-4 linkage. In these studies, there has been considerable focus on the effect that functionalizing groups can have on bond dissociation energies. In light of these studies, we added a hydroxyl group to the α-carbon in the β-O-4 dimer and repeated the steered MD studies with two trajectories at each of the 25 combinations of pulling points. In this case, the presence of the α-hydroxy changes the stereocenter for the β-O-4 linkage (see Fig. 3) from R to S, although the geometry is unchanged. The mechanisms for cleavage are unchanged from those observed in the absence of the α-hydroxy functionalization (see Fig. 5), consistent with previous observations that this functionalization does not strongly alter homolytic bond dissociation energies[47]. However, we do observe seven more breaking events for an overall 14% higher cleavage frequency. Higher numbers of trajectories at additional force thresholds would likely be necessary to ascertain if the increased cleavage frequency observed in the functionalized β-O-4 linkage over the pristine linkage is significant. Indeed, homolytic bond dissociation energy calculations would likely be a more suitable tool for identifying subtle changes in the bond strength of linkages upon functionalization. The force-modified molecular dynamics approach is instead more suitable for sampling possible mechanisms of bond cleavage and subsequent dynamic rearrangement following cleavage.

The low-abundance (*ab*=3%) β-1 linkage is relatively analogous to β-O-4, but here the β carbon of the first monomer is bonded directly to the phenyl ring of the second monomer, rather than through an ether linkage. The absence of an easily cleaved ether bond reduces the fragmentation frequency to *cf*=18%, with the most commonly observed fragmentation pathway involving homolytic cleavage between the α and β carbon. A second, minor cleavage pathway involves direct homolytic cleavage of the bond between the β carbon and the second phenyl ring, leaving a phenyl radical and an alkyl radical at the β position. In one of the two trajectories following this second pathway, the alkyl radical proceeded to abstract a hydrogen atom from the neighboring γ carbon, leading to the formation of a C-O double bond. This event was followed

by the transfer of the γ-hydroxyl hydrogen to the phenyl radical, yielding closed-shell phenyl and aldehyde fragments (see Supporting Information). While the highly abundant β-O-4 linkages will be the focus of our study of larger oligomers, we have thus also identified bond-cleavage patterns in diverse linkages for further comparison and to identify the relative variability in possible fragmentation pathways.

Of all the linkages considered, the β-β linkage (*ab*=3.5%) had the highest occurrence (*cf*=92%) of bond cleavage. This linkage is symmetric and consists of two five-membered rings fused at the β-carbons of each monomer, with the γ-hydroxyl group of each monomer forming an ether bond to the α carbon of the other monomer to close the five-membered ring. We consistently observe a simultaneous, double electrocyclic reaction, in which the β and γ carbons of both monomers are released as a free 1,3-butadiene molecule. Each monomer retains the γ-hydroxyl oxygen of the other monomer to form two neutral aldehyde-terminated fragments (Fig. 6). In contrast to β-β, the moderately abundant (*ab*=10%) β-5 linkage has few cleavage events (*cf*=4%) where the five-membered ring opens, with the γ carbon and its attached hydroxyl group is released as a free formaldehyde molecule, but further fragmentation to monomers does not occur (See Supporting Information). These contrasting cases suggest that the dissociation of linkages should be investigated carefully on a case-by-case basis, and a follow-up study will be focused on using more detailed charge and bonding analysis to reveal structure-property relationships in these cleavage events when in the presence of model catalysts.

4b. Trimer studies

Dibenzodioxocin is a linkage formed from three monomers that is characterized by an eight-membered ring comprised of two 5-5 linked phenyl groups and a third monomer attached to the first two monomers via β-O-4 and α-O-4 linkages, respectively. Relatively low breaking frequency (*cf*=16%) in dibenzodioxocin is likely due to the fact that differing simulations contained different pulling point and attachment point combinations that distribute the force across different parts of the molecule distinctly, with a large subset effectively stressing only the 5-5 linkage (see more discussion in Sec. 4c). We have previously observed the absence of cleavage events in the case of pure 5-5 dimers. For dibdenzodioxocin, initial cleavage occurs at one of the ether linkages. However, notably, we observed in one case that initial cleavage of both ether linkages leads to release of one monomer (see Supporting Information), with the

typically inert 5-5 link between the remaining dimeric fragment breaking apart in the ensuing rearrangement (Fig. 7). Distortion of the rings is apparent in Fig. 7 due to the fact that the initial double bond cleavage disrupts aromaticity of the phenyl rings, and this electronic rearrangement likely facilitates cleavage of the normally inert C-C bond. Notably, once the ether linkages are cleaved, there is no formal pulling force across the molecule any longer. The dynamics continues with the energy present in the system following bond cleavage and the remaining fragment is pulled on a single AP towards a PP. While the molecule has translational velocity, this portion of the simulation approximates standard *ab initio* molecular dynamics. Following this observation of β-O-4-induced 5-5 cleavage, we carried out several simulations on 5-5/β-O-4/5-5 tetramers. We observed cleavage to occur 100% of the time at the β-O-4 linkage with no subsequent rearrangement of 5-5 bonds. This result suggests that the conditions required for 5-5 cleavage in mixed linkage models are relatively specific to the strain and local chemistry. Study of mixed 5-5 and β-O-4 linkages in rings, linear, and branched chains in order to identify whether we can induce 5-5 cleavage through cleavage of neighboring β-O-4 linkages will be the focus of future work.

The final minimal linkage considered here, spirodienone, differed from the other linkages in that instead of one or two distinct fragmentation pathways, this linkage was observed to exhibit 23 distinct cleavage pathways. Because there are several different bonds in this linkage susceptible to force-initiated cleavage, a variety of intermediate species appeared in the course of the dynamics runs. While their abundance is relatively low, the three-monomer linkages (spirodienone and dibenzodioxocin) are potentially important as they are the origin of cross-linking that contributes to the general difficulty in the valorization of lignin biomass. Of these two, spirodienone is much more susceptible to cleavage (*cf*=69% vs. 16% in dibenzodioxocin), and thus offers the greater potential as an avenue toward unraveling the polymer. Nevertheless, spirodienone is probably the least well-known of lignin linkage structures, having only been discovered by NMR in 2001[62]. Future studies are underway aimed at identifying the most important cleavage pathways, and determining how the reactive intermediates involved in these pathways would behave in the presence of other adjacent linkages. Spirodienone remains emblematic of the complex chemistry present in lignin that has still yet to be fully understood.

4c. Dependence of cleavage on simulation conditions

We previously noted that cleavage frequency is not strictly comparable to bond dissociation energy and force dependent profiles are more likely to give useful statistics. Bond cleavage events are inherently sensitive to the relative orientation of the two attachment points on the molecule that we choose during a pulling study. In the case of each dimer or trimer, 25 possible pulling point combinations were selected, and two trajectories were run for each attachment point combination. From a discovery perspective, one advantage to our steered MD approach is that different attachment points may bias towards distinct cleavage mechanisms, permitting identification of pathways that might have been excluded based on chemical intuition. This variability led to observation of 23 unique fragmentation pathways in the spirodienone linkage. However, for cases where only a few pathways were observed, it is also useful to note the dependence of cleavage on the combination of attachment points in order to identify whether certain combinations apply uneven or insufficient stress to the cleaving bond.

For analysis, the type of attachment point combination is classified by whether the attachment point is ortho, meta, or para to the phenyl ring carbon that is closest to the linking bond (recall that this carbon is excluded from the attachment points). The strictly para/para and para/meta combinations are designated as more longitudinal force being applied along the axis of the cleaving bond and correspond to 10 out of 50 trajectories for each dimer. The most transverse applied forces, which would be equivalent to bending or torqueing the cleaving bond, correspond to ortho/ortho or meta/ortho combinations (24 out of 50 trajectories for each dimer). The remaining meta/meta and ortho/para attachment point configurations are classified as intermediate (16 out of 50 trajectories for each dimer). The cleavage frequencies within each class of attachment points is provided in Table 1, and we note that these frequencies must be reweighted by the number of trajectories in each class in order to compare to the total cleavage frequency provided earlier in the text. Cleavage statistics on dibenzodioxocin are also provided in two forms: 1) the total cleavage for longitudinal (32 out of 112 trajectories), intermediate (8 out of 112 trajectories), and transverse (72 out of 112 trajectories) and 2) delineated by attachment points across each individual linkage (5-5, α-O-4, or β-O-4). The overall statistics across the lignin models indicate that bond cleavage events are distributed across all types of applied force: 32% for longitudinal (L), 38% for intermediate (I), and 33% for transverse (T).

Results on individual models, however, suggest that different types of applied forces are more suitable for different types of linking bonds. Bending forces are more effective in β-1 (0% L, 25% I, and 21% T *cf*) For both β-5 and 4-O-5, cleavage frequency is too low to provide a definitive statement but is also suggestive of a preference for intermediate and transverse applied forces, also suggesting that more trajectories could be run in these combinations in order to enhance sampling of pathways corresponding to breaking events in future work. In the β-β linkage, this trend is reversed (100% L, 81% I, and 75% T *cf*), though we note very high overall cleavage frequencies. Notably, the β-β bond itself is at a slight angle with respect to the closest phenyl ring carbons, and a probable mechanism is that the longitudinal force applies the most stress to the outer rings that the β-β bond bisects. The dibenzodioxocin trimer also prefers longitudinal force overall, with longitudinal and transverse being the predominant method for cleaving α-O-4 (42% L, 50% I, 29% T *cf*) as well as β-O-4 (17% L 0% I, 8% T *cf*) linkages. Applying force directly in any combination to the 5-5 linkage of dibenzodioxocin did not lead to cleavage events, consistent with observations in the 5-5 dimer. Observations on the β-O-4 linkage are mixed and would require more statistics to interpret whether differences between the unfunctionalized and α-hydroxy β-O-4 are significant. Namely, we previously noted a 14% increase in overall cleavage frequency in the presence of an α-hydroxy for β-O-4, and this appears to shift the preference from transverse for standard β-O-4 (40% L, 38% I, 75% T) to longitudinal for those with α-OH present (80% L, 75% I, 71% T). Overall, both linkages show cleavage regardless of the type of force applied. The overall and individual linkage statistics suggest that all forms of applied force will be suitable for discovery of cleavage pathways, though in some cases, more sampling of applied intermediate or transverse forces would be ideal for maximizing the number of cleavage pathways observed.

4d. Hexamer studies

We now shift focus to a different screening approach from those observed with minimal models to identifying the dynamic effects of bond cleavage on larger-scale oligomers. To our knowledge, hexameric models of lignin containing β-O-4 linkages represent the largest models of lignin that have been studied with first principles simulations. However, there have been some successful efforts in experimentally synthesizing such compounds[83-84] in order to better

understand the biological synthesis of lignin during plant growth. Our initial motivation for studying larger models of the well-studied β-O-4 ether linkage was to identify whether bond-breaking events propagate in a manner at all analogous to our previous observations with low-ceiling temperature polymers[59]. Similarly, we screened for breaking events at a range of lowered force thresholds (as low as 1.0 nN and as high as 3.5 nN) in order to identify whether cleavage events occurred at lower forces as they did in other polymers we have previously studied. Additionally, the force-dependent breaking ratio (i.e. how many simulations lead to cleaved products at a given force) gives us information about the minimum force to cleave a bond in the presence or absence of a catalyst. This information allows us to identify better catalysts as those that will lower the force threshold at which bond cleavage occurs. Such studies also permit dynamic rearrangement after the catalytic cleavage, allowing for identification of any side reactions or other unexpected steps not normally considered in more commonly employed minimum energy pathway studies of catalysis.

While we did observe some double and triple breaking events in the hexameric models, these cleavage events were typically simultaneous and corresponded to equivalent breaking events occurring at either end of the molecule. This multiple-cleavage event mechanism was primarily observed at the highest forces (3.5 nN) employed. The cleavage threshold for breaking events was between 2.0 and 2.5 nN with a cleavage frequency of around 40% for 2.25 nN pulling force (model of the hexamer and force-dependent cleavage-frequency shown in Fig. 8). We did not screen for force-dependent breaking thresholds in the earlier minimal dimer models where we instead aimed to maximize bond-breaking. As in the case of the dimer, the hexamers here have R stereocenters (see Fig. 3 for stereocenter indication on dimer model). Regardless of force applied, we note that there is no change in the mechanism observed for bond cleavage. While in small molecules, it has been observed that mechanical force can subtly change ring-opening mechanisms in violation of the Woodward-Hoffman rules[55], our observation that very low forces lead to the same cleavage patterns suggest that ether bond cleavage is unperturbed by the use of force-modified molecular dynamics. The only alternative pathway observed in the hexamer but absent in the dimer was formation of a phenol and epoxide at 2.25 nN. Here, we have sampled a greater number of possible initial configurations and dynamics by running at least 25 trajectories at each force and we have five copies of each linkage in the hexamer, versus one in the dimer. In

contrast to our observations in β-O-4 hexamers, random hexamers studied with high temperature (1650-2300 K) reactive force field molecular dynamics simulations[61] yielded degradation to a wider array of products, including a number of polycyclic compounds. These compounds were traced to the rearrangement after cleavage of other bonds such as 5-5 and β-5 not present in our hexamer models.

Following confirmation that the hexameric models of β-O-4 ether linkages behaved largely similar to the dimeric models, we then considered whether we could identify mechanisms by which a model acid or base catalyst might alter the cleavage events in this oligomer. We continued to work with the larger model for two reasons: 1) use of the hexamer allowed us to probe whether acid/base catalyzed mechanisms were sensitive to the location of the cleaving bond in the oligomer and 2) hexamer models break at lower force profiles, giving us access to a wider range of forces over which we can assess cleavage frequency than in the case of the smaller dimers. In order to probe the role of the model acid in catalyzing bond cleavage, we placed an acid (hydronium ion) at each of five possible sites adjacent to the ether linkage (see Fig. 8). Then we ran sampling dynamics of at least five trajectories for each placement. We observe a significant reduction in the force at which cleavage first occurs (*cf* > 60% at 1.5 nN) when in the presence of the acid. However, the major chemical pathways (see Fig. 5 and Supporting Information) are largely unchanged with respect to the uncatalyzed hexamer. The major uncatalyzed pathways in the presence of an additional proton form a phenol/carbocation combination or a protonated phenol/enol by analogy. There is a bit more variety in the subsequent rearrangements for the acid case than in the uncatalyzed simulations, since the intermediates are fairly unstable. Formation of a protonated epoxide is a common rearrangement observed in our trajectories. Such species may be of use for further study in identifying the structures formed during recently successful experimental observations of lignin depolymerization by formic acid[20]. We also considered whether functionalization by α-hydroxy groups would have a larger effect in the case of hexamers both with and without acid. In select acid catalysis pathways, protonation occasionally occurred at the hydroxyl rather than at the ether. This latter observation is more consistent with the pathways proposed by Sturgeon et al.[19], which begin from the assumption of the protonation of the additional hydroxyl functional group. The discrepancy here arises in that we preferentially placed the hydronium ion adjacent to the

ether bond, enhancing the likelihood of a protonated ether bond. Our simulations definitively demonstrate that protonation of the ether bond lowers the barrier for cleavage of the β-O-4 linkage. However, it might be interesting to carry out more simulations that start from β-O-4 models that have protonated α-hydroxyl functional groups in order to identify whether biasing instead towards that mechanism will lower the barrier for cleavage in a manner that is distinct from the ether bond protonation mechanism that predominates in our study. Aside from this alternate pathway, both acid-catalyzed and uncatalyzed hexamer cleavage patterns were unchanged by α-hydroxy functionalization.

For the study of base-mediated catalysis, we used the tertbutoxide anion, which is a strong base but poor nucleophile. By using a poor nucleophile, we thus prevent observation of direct nucleophilic attack in our simulations. As in the acid case, we see reduction in the force threshold at which bond cleavage occurs, but this effect is not as pronounced (*cf* ~ 20% at 1.5 nN). Overall, the force-dependent profiles show that at higher forces (2.0 nN-2.25 nN) the base catalyst cleavage frequencies nearly approach the acid catalyst but not quite, suggesting that the base is acting as a slightly weaker catalyst for ether bond cleavage. Nevertheless, both acid and base catalyzed pathways produce a significant majority of cleaved pathways at intermediate forces (2.0 nN-2.25 nN) where the uncatalyzed pathways only have cleavage in 40% of all trajectories at the higher 2.25 nN force and only reach 100% cleavage at 3.0 nN. In the base, the cleavage mechanism largely occurs via deprotonation of the nearby γ-hydroxyl, creating a good nucleophile for intramolecular attack leading to cyclization and loss of the ether leaving group. This mechanism is the same as that proposed in previous base-catalyzed experimental studies (scheme 3 in Ref. [85]). In the case of position #4, we observe some different behavior. When the base is not positioned well to abstract a proton from the hydroxyl, cleavage occurs as in the uncatalyzed case, but with subsequent attack of the base on the radical fragment (see Supporting Information). There are again, as in the uncatalyzed case, a few double cleavage events. For one double cleavage event, the α-β C-C bond is cleaved, which is the only time a β-O-4-containing lignin model breaks somewhere other than at the ether bond in our simulations. This C-C bond cleavage also occurs down the chain, not at the position where the base is initially placed. Such unusual dynamics in base-catalyzed lignin models will be probed with future work in which we also consider good nucleophilic bases and those that have been observed to be effective catalysts

experimentally[18]. We also note that α-hydroxy functionalization had no discernible effect on the base-catalyzed mechanisms with respect to the pristine β-O-4 models.

5. Conclusions

We have demonstrated the first force-based *ab initio* molecular dynamics screening approach for the chemical discovery of bond cleavage events. Our method builds on the already well-established tools for identifying mechanochemical bond cleavage in polymers in the chemistry community. However, we have turned this successful approach on its head to discover the heterogeneity in products that can be formed when any kind of bond cleavage occurs in the highly heterogeneous lignin biopolymer. While microkinetic models have been quite successful in modeling the homogeneous cellulose polymer with models that are smaller than the ones we have considered in our study, understanding how to utilize, upgrade, and catalytically convert lignin into value-added products is an ongoing challenge.

Our approach has permitted the confirmation of previous observations, namely that ether bonds cleave readily in lignin polymers and that biphenyl linkages are more recalcitrant. Additionally, we have carried out, to our knowledge, the first screen of all known model linkages of lignin, including two branched linkages, using one first principles computational screen. This breadth comes at a natural cost of reduced detail with respect to analysis on any single linkage. Future work will allow us to provide more insights into the cleavage of linkages in lignin both by examining more commonly studied effects such as the impact of ring functionalization on bond cleavage and more electronic-structure-based analysis on fragmentation patterns. Nevertheless, with this newly introduced approach, we have identified for the first time that spirodienone branching linkages can fragment into many possible products with high frequency of cleavage. Additionally, we have identified in one case where breaking an "easy" to break ether bond also results in the spontaneous cleavage of a harder to break biphenyl-like bond. In the case of larger models of the polymer, we confirmed that cleavage events are unchanged by chain lengthening, but that force-dependent screens can provide a handle for identifying the relative activity and mechanism of a class of catalysts. Our rapid GPU-accelerated density functional theory approach has permitted the study of the dynamics of thousands of individual bond cleavage events. Such sampling and screening is crucial in lignin where the high heterogeneity of the structure

necessitates sampling. Notably, we have only identified likely chemical mechanisms and fragmentation patterns under the circumstance in which cleavage occurs. We have not yet carried out studies of the enthalpies of the bond-dissociation energies, but we have instead used *ab initio* molecular dynamics to explore a force-modified potential energy surface where the bond cleavage is barrierless.

Future work will be focused towards the development for catalyst screens to lower enthalpic and free energy barriers for the dissociation mechanisms we have observed in model linkages. Although our priority has been in the evaluation of dynamic rearrangement following cleavage, bond-dissociation energies remain a common point of comparison for evaluating properties of lignin models. Future work will also focus on comparison of our dynamic approach to bond dissociation energies by carrying out more fine-grained force-dependent cleavage statistics. We are also interested in identifying ways to generalize the observations we have made in the dibenzodioxocin linkage to identify how to destabilize the recalcitrant biphenyl-like 5-5 linkages in lignin by modifying and destabilizing the most probable adjacent molecular fragments. Much work is left to be done in still discovering the organic chemistry and electronic structure of lignin model compounds and lignin polymers. While commercialization is already underway of the treatment of lignin-derived bio-oil, there remain many mysteries left to unravel in the complex heterogeneous polymers that make up biomass.

Supporting Information

(i) Schematics of mechanisms for 5-5, β-1, β-5, and 4-O-5 rupture in dimer models, (ii) snapshots from initial β-O-4-like cleavage of dibenzodioxocin, (iii) additional hexamer acid-and base- catalyzed breaking pathways, (iv) extended bond-breaking statistics for various linkages of dimers and trimers, and (v) comparison of variation in C-C bond lengths across molecular dynamics trajectory. This material is available free of charge via the Internet at http://pubs.acs.org.

Corresponding Author

*E-mail: hjkulik@mit.edu

Acknowledgements

The authors gratefully acknowledge Adam H. Steeves, the Hoffman group at Cornell University, the Martinez group at Stanford University, and the Roman group at MIT for helpful conversations. B.D.M. and H.J.K. were supported by a Reed grant from the Research Support Corporation (MIT). H.W.Q. is supported by a Department of Energy Computational Science Graduate Fellowship (DOE-CSGF). H.J.K. holds a Career Award at the Scientific Interface from the Burroughs Wellcome Fund.

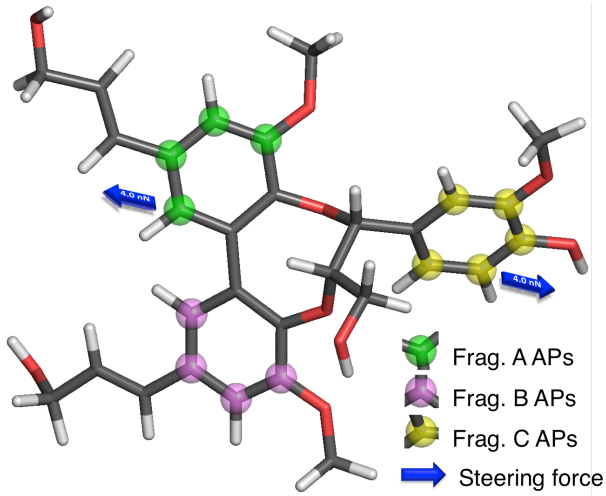

Figure 1. Example trimeric linkage (dibenzodioxocin) with possible sites for attachment points (labeled in green, pink, and yellow spheres for fragments A, B, and C, as indicated in the legend). Two attachment points are pulled with a steering force to a distant pulling point along the blue force vector indicated by a blue arrow.

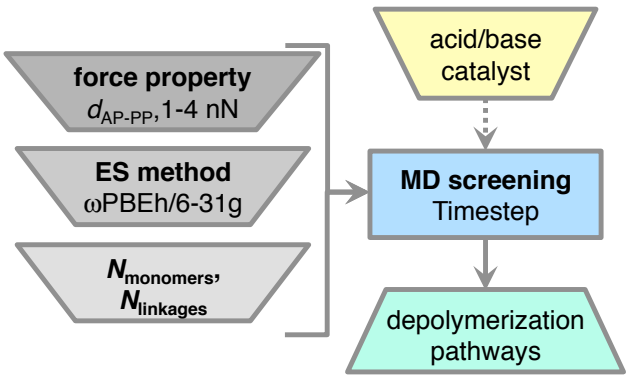

Figure 2. Flowchart for enhanced screening approach to identify depolymerization pathways in lignin. Tunable screening parameters are indicated on the left-hand side in gray trapezoids, while the main computational effort is the MD screening to yield depolymerization pathways, possibly in the presence of model catalysts (indicated by dashed arrow).

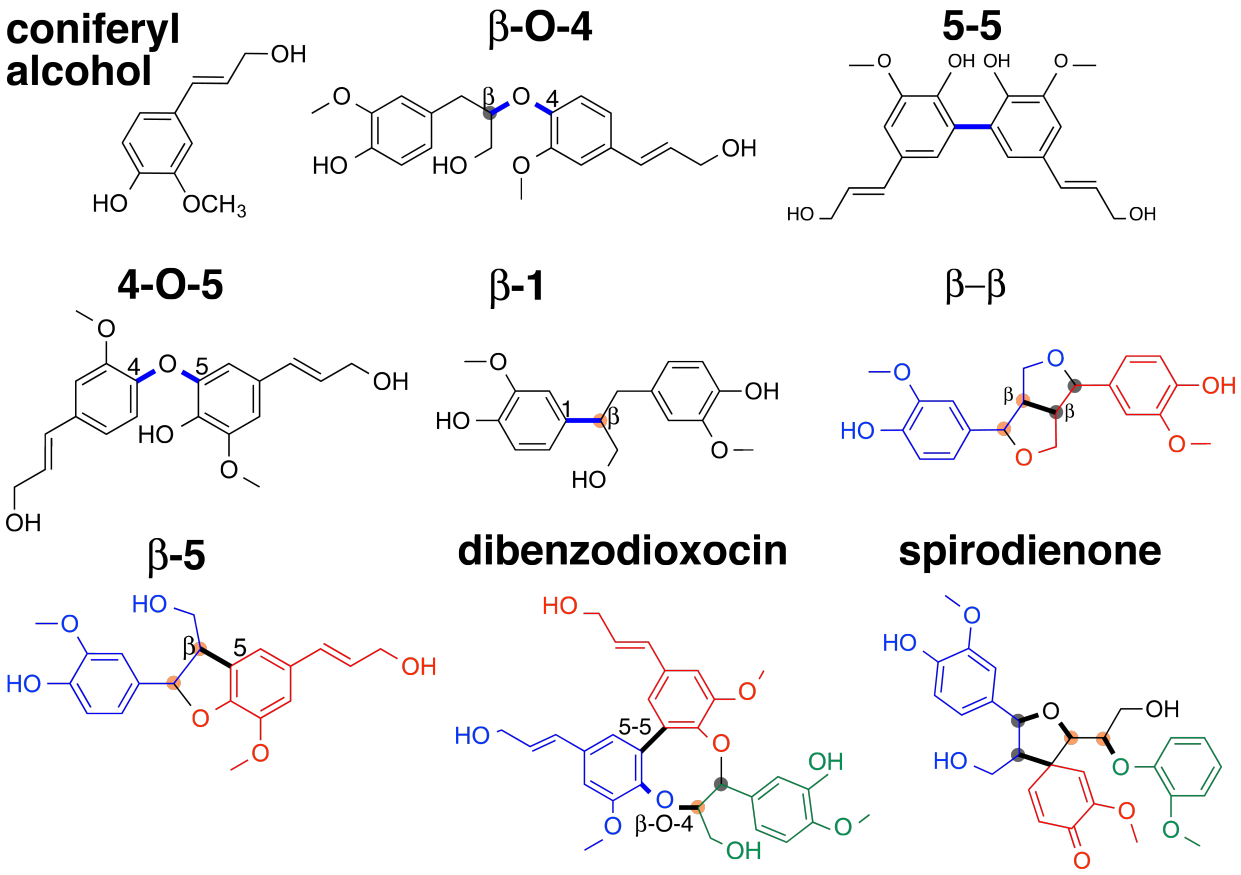

Figure 3. Structure of coniferyl alcohol monolignol and eight lignin linkages formed by the monolignol. Single-bond, dimeric linkages are indicated with black structures and linking bonds indicated in blue. Multi-bond dimeric and trimeric linkages are indicated with red, blue, and green color to designate each monomer unit and key linking bonds highlighted with thickened black lines. Stereochemistry is indicated on each model by a gray circle for R stereocenters and an orange circle for S stereocenters.

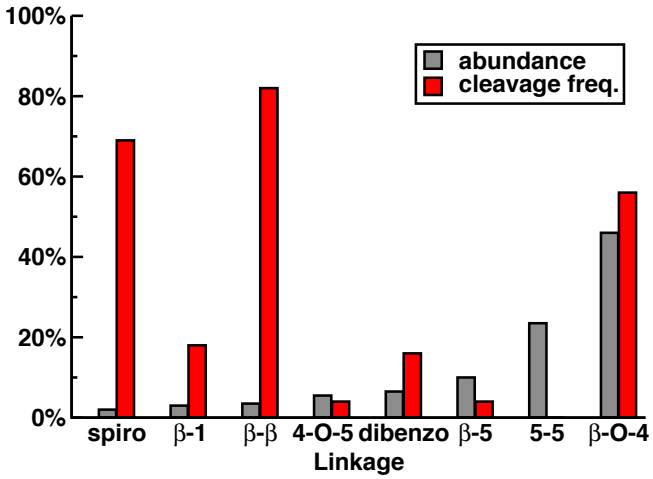

Figure 4. Percentage of natural abundance (gray bars) as well as observed cleavage frequency for eight lignin linkages (red bars). The abundance sums overall to 100% while the cleavage frequency may be individually up to 100% for a given linkage. Spirodienone is abbreviated as spiro, and dibenzodioxocin is labeled dibenzo.

Scheme 1.

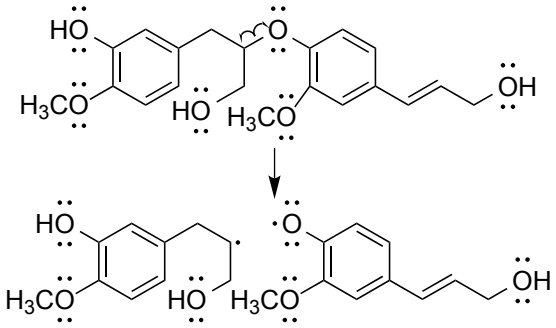

Scheme 2.

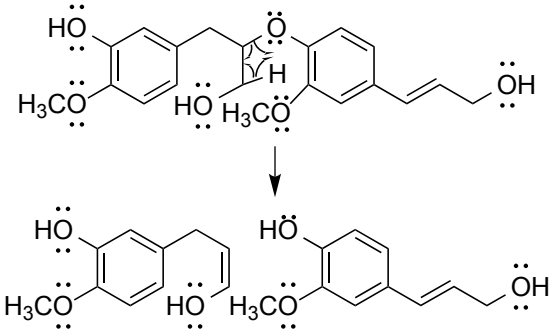

Scheme 3.

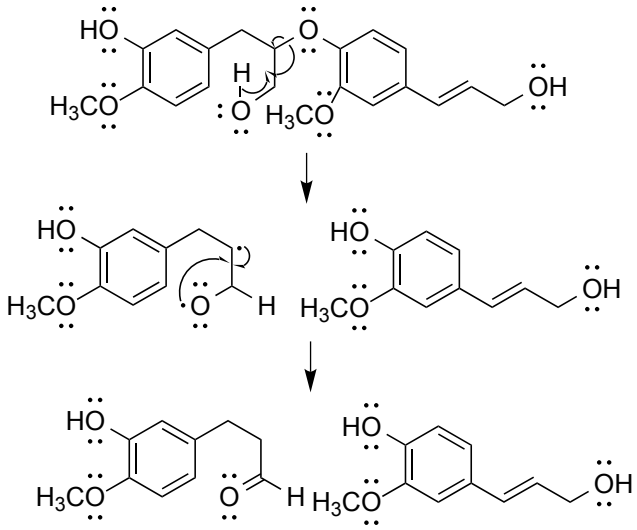

Figure 5. Three observed mechanisms for homolytic cleavage of β-O-4 linkage in coniferyl alcohol dimers or hexamers. The first case involves dissociation to radical products, while the latter two exhibit proton transfer to lead to closed shell fragments.

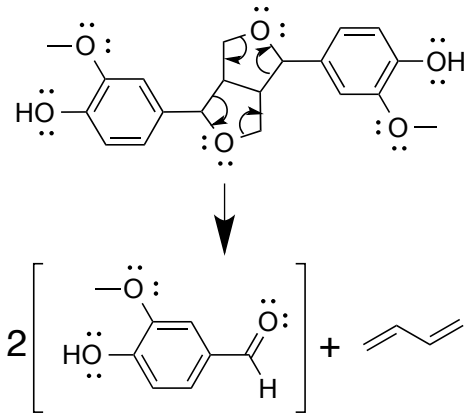

Figure 6. Primary mechanism of β-β dimer linkage cleavage observed in 4.0 nN steered MD. A double electrocyclic ring cleavage leads to a free 1,3-butadiene molecule and two neutral aldehyde-terminated monomers.

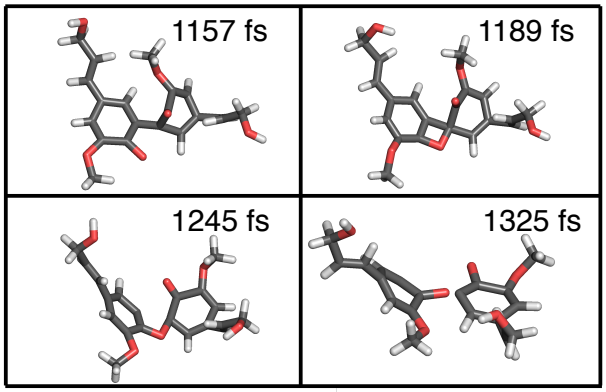

Figure 7. Snapshots from the cleavage of a 5-5-like bond in the dibenzodioxocin sequential cleavage pathway labeled with the timing of each frame from the steered molecular dynamics run. No force is being formally applied across the molecule.

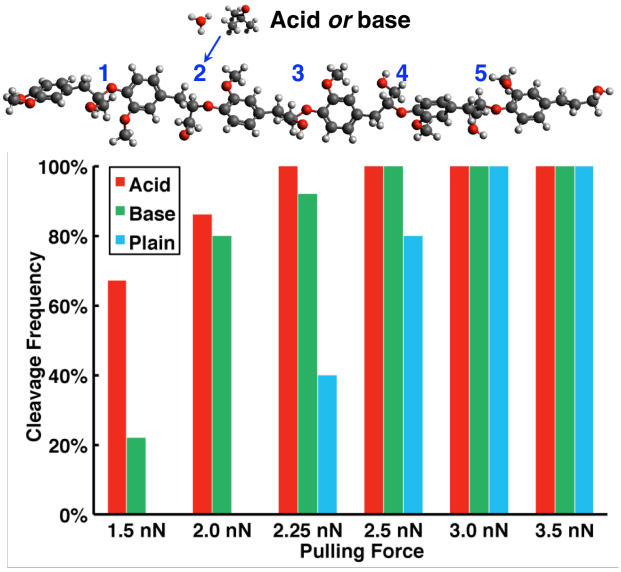

Figure 8. (Top) Model of a hexamer of lignin with the five linkages indicated and numbered in blue. The acid (hydronium) and base (tertbutoxide) model structures are also shown alongside their relative placement during dynamics. (Bottom) Steering-force dependence of the cleavage statistics for acid, base, and uncatalyzed β-O-4 hexamer lignin models obtained at forces ranging from 1.5 nN to 3.5 nN.

Table 1. Cleavage frequency for representative lignin dimers and trimers classified by type of force applied to the linkage. The dibenzodioxocin trimer cleavage statistics are also subdivided by the different types of linkages being stressed.

Linkage	Longitudinal	Intermediate	Transverse
β-O-4	40%	38%	75%
β-O-4 w/ α-OH	80%	75%	71%
4-O-5	0%	6%	4%
β -1	0%	25%	21%
β - β	100%	81%	75%
β -5	0%	0%	8%
dibenzodioxocin	22%	25%	13%
5-5	0%	--	0%
α-O-4	42%	50%	29%
β-O-4	17%	0%	8%
Overall	32%	38%	33%

TOC graphic

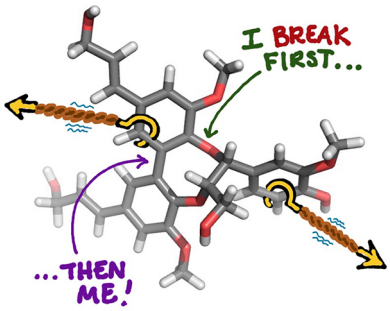

References

1. Turkenburg, W. C.; Beurskens, J.; Faaij, A.; Fraenkel, P.; Fridleifsson, I.; Lysen, E.; Mills, D.; Moreira, J. R.; Nilsson, L. J.; Schaap, A., Renewable Energy Technologies. *World energy assessment: Energy and the challenge of sustainability* **2000**, 219-272.
2. Klass, D. L., Biomass for Renewable Energy and Fuels. *Encyclopedia of energy* **2004,** *1*, 193-212.
3. Gayubo, A. G.; Valle, B.; Aguayo, A. T.; Olazar, M.; Bilbao, J., Pyrolytic Lignin Removal for the Valorization of Biomass Pyrolysis Crude Bio-Oil by Catalytic Transformation. *J. Chem. Technol. Biotechnol.* **2010,** *85*, 132-144.
4. Bruijnincx, P. C. A.; Weckhuysen, B. M., Biomass Conversion: Lignin up for Break-Down. *Nature Chem.* **2014,** *6*, 1035-1036.
5. Linger, J. G.; Vardon, D. R.; Guarnieri, M. T.; Karp, E. M.; Hunsinger, G. B.; Franden, M. A.; Johnson, C. W.; Chupka, G.; Strathmann, T. J.; Pienkos, P. T., et al., Lignin Valorization through Integrated Biological Funneling and Chemical Catalysis. *Proc. Natl. Acad. Sci. U. S. A.* **2014,** *111*, 12013-12018.
6. Ragauskas, A. J.; Beckham, G. T.; Biddy, M. J.; Chandra, R.; Chen, F.; Davis, M. F.; Davison, B. H.; Dixon, R. A.; Gilna, P.; Keller, M., et al., Lignin Valorization: Improving Lignin Processing in the Biorefinery. *Science* **2014,** *344*.
7. Strassberger, Z.; Tanase, S.; Rothenberg, G., The Pros and Cons of Lignin Valorisation in an Integrated Biorefinery. *RSC Adv.* **2014,** *4*, 25310-25318.
8. Dutta, S.; Wu, K. C. W.; Saha, B., Emerging Strategies for Breaking the 3D Amorphous Network of Lignin. *Catal. Sci. Technol.* **2014,** *4*, 3785-3799.
9. Kersten, S.; Garcia-Perez, M., Recent Developments in Fast Pyrolysis of Ligno-Cellulosic Materials. *Curr. Opin. Biotechnol.* **2013,** *24*, 414-420.
10. Zhou, X.; Nolte, M. W.; Shanks, B. H.; Broadbelt, L. J., Experimental and Mechanistic Modeling of Fast Pyrolysis of Neat Glucose-Based Carbohydrates. 2. Validation and Evaluation of the Mechanistic Model. *Ind. Eng. Chem. Res.* **2014,** *53*, 13290-13301.
11. Azadi, P.; Carrasquillo-Flores, R.; Pagan-Torres, Y. J.; Gurbuz, E. I.; Farnood, R.; Dumesic, J. A., Catalytic Conversion of Biomass Using Solvents Derived from Lignin. *Green Chem.* **2012,** *14*, 1573-1576.
12. Johnson, C. W.; Beckham, G. T., Aromatic Catabolic Pathway Selection for Optimal Production of Pyruvate and Lactate from Lignin. *Metab. Eng.* **2015,** *28*, 240-247.
13. Zaheer, M.; Kempe, R., Catalytic Hydrogenolysis of Aryl Ethers: A Key Step in Lignin Valorization to Valuable Chemicals. *ACS Catal.* **2015,** *5*, 1675-1684.
14. Prasomsri, T.; Shetty, M.; Murugappan, K.; Román-Leshkov, Y., Insights into the Catalytic Activity and Surface Modification of Moo 3 During the Hydrodeoxygenation of Lignin-Derived Model Compounds into Aromatic Hydrocarbons under Low Hydrogen Pressures. *Energy Environ. Sci.* **2014,** *7*, 2660-2669.
15. Gilormini, P.; Richaud, E.; Verdu, J., A Statistical Theory of Polymer Network Degradation. *Polymer* **2014,** *55*, 3811-3817.
16. Zakzeski, J.; Jongerius, A. L.; Bruijnincx, P. C. A.; Weckhuysen, B. M., Catalytic Lignin Valorization Process for the Production of Aromatic Chemicals and Hydrogen. *ChemSusChem* **2012,** *5*, 1602-1609.

17. Roberts, V. M.; Stein, V.; Reiner, T.; Lemonidou, A.; Li, X.; Lercher, J. A., Towards Quantitative Catalytic Lignin Depolymerization. *Chem. Eur. J.* **2011,** *17*, 5939-5948.
18. Xia, G.-G.; Chen, B.; Zhang, R.; Zhang, Z. C., Catalytic Hydrolytic Cleavage and Oxy-Cleavage of Lignin Linkages. *J. Mol. Catal. A: Chem.* **2014,** *388–389*, 35-40.
19. Sturgeon, M. R.; Kim, S.; Lawrence, K.; Paton, R. S.; Chmely, S. C.; Nimlos, M.; Foust, T. D.; Beckham, G. T., A Mechanistic Investigation of Acid-Catalyzed Cleavage of Aryl-Ether Linkages: Implications for Lignin Depolymerization in Acidic Environments. *ACS Sustainable Chem. Eng.* **2014,** *2*, 472-485.
20. Rahimi, A.; Ulbrich, A.; Coon, J. J.; Stahl, S. S., Formic-Acid-Induced Depolymerization of Oxidized Lignin to Aromatics. *Nature* **2014,** *515*, 249-252.
21. Wen, J.-L.; Yuan, T.-Q.; Sun, S.-L.; Xu, F.; Sun, R.-C., Understanding the Chemical Transformations of Lignin During Ionic Liquid Pretreatment. *Green Chem.* **2014,** *16*, 181-190.
22. Feghali, E.; Cantat, T., Unprecedented Organocatalytic Reduction of Lignin Model Compounds to Phenols and Primary Alcohols Using Hydrosilanes. *Chem. Commun. (Cambridge, U. K.)* **2014,** *50*, 862-865.
23. Nguyen, J. D.; Matsuura, B. S.; Stephenson, C. R. J., A Photochemical Strategy for Lignin Degradation at Room Temperature. *J. Am. Chem. Soc.* **2014,** *136*, 1218-1221.
24. Fujimoto, A.; Matsumoto, Y.; Chang, H.-M.; Meshitsuka, G., Quantitative Evaluation of Milling Effects on Lignin Structure During the Isolation Process of Milled Wood Lignin. *J. Wood Sci.* **2005,** *51*, 89-91.
25. Hanson, S. K.; Baker, R. T.; Gordon, J. C.; Scott, B. L.; Thorn, D. L., Aerobic Oxidation of Lignin Models Using a Base Metal Vanadium Catalyst. *Inorg. Chem.* **2010,** *49*, 5611-5618.
26. Hicks, J. C., Advances in C-O Bond Transformations in Lignin-Derived Compounds for Biofuels Production. *J. Phys. Chem. Lett.* **2011,** *2*, 2280-2287.
27. Nichols, J. M.; Bishop, L. M.; Bergman, R. G.; Ellman, J. A., Catalytic C-O Bond Cleavage of 2-Aryloxy-1-Arylethanols and Its Application to the Depolymerization of Lignin-Related Polymers. *J. Am. Chem. Soc.* **2010,** *132*, 12554-12555.
28. Sergeev, A. G.; Hartwig, J. F., Selective, Nickel-Catalyzed Hydrogenolysis of Aryl Ethers. *Science* **2011,** *332*, 439-443.
29. Son, S.; Toste, F. D., Non-Oxidative Vanadium-Catalyzed C-O Bond Cleavage: Application to Degradation of Lignin Model Compounds. *Angew. Chem., Int. Ed.* **2010,** *49*, 3791-3794.
30. Bugg, T. D. H.; Ahmad, M.; Hardiman, E. M.; Singh, R., The Emerging Role for Bacteria in Lignin Degradation and Bio-Product Formation. *Curr. Opin. Biotechnol.* **2011,** *22*, 394-400.
31. Pandey, M. P.; Kim, C. S., Lignin Depolymerization and Conversion: A Review of Thermochemical Methods. *Chem. Eng. Technol.* **2011,** *34*, 29-41.
32. Song, Q.; Wang, F.; Cai, J.; Wang, Y.; Zhang, J.; Yu, W.; Xu, J., Lignin Depolymerization (Ldp) in Alcohol over Nickel-Based Catalysts Via a Fragmentation–Hydrogenolysis Process. *Energy Environ. Sci.* **2013,** *6*, 994-1007.
33. Parsell, T.; Yohe, S.; Degenstein, J.; Jarrell, T.; Klein, I.; Gencer, E.; Hewetson, B.; Hurt, M.; Kim, J. I.; Choudhari, H., et al., A Synergistic Biorefinery Based on Catalytic Conversion of Lignin Prior to Cellulose Starting from Lignocellulosic Biomass. *Green Chem.* **2015,** *17*, 1492-1499.
34. Huber, G. W.; Iborra, S.; Corma, A., Synthesis of Transportation Fuels from Biomas: Chemistry, Catalysts, and Engineering. *Chem. Rev.* **2006,** *106*, 4044-4098.

35. Kim, S.; Chmely, S. C.; Nimos, M. R.; Bomble, Y. J.; Foust, T. D.; Paton, R. S.; Beckham, G. T., Computational Study of Bond Dissociation Enthalpies for a Large Range of Native and Modified Lignins. *J. Phys. Chem. Lett.* **2011,** *2*, 2846-2852.
36. Parthasarathi, R.; Romero, R. A.; Redondo, A.; Gnanakaran, S., Theoretical Study of the Remarkably Diverse Linkages in Lignin. *J. Phys. Chem. Lett.* **2011,** *2*, 2660-2666.
37. Elder, T., Quantum Chemical Determination of Young's Modulus of Lignin. Calculations on a Beta-O-4' Model Compound. *Biomacromolecules* **2007,** *8*, 3619-3627.
38. Chen, W.; Lickfield, G. C.; Yang, C. Q., Molecular Modeling of Cellulose in Amorphous State. Part I: Model Building and Plastic Deformation Study. *Polymer* **2004,** *45*, 1063-1071.
39. Eichhorn, S. J.; Young, R. J.; Davies, G. R., Modeling Crystal and Molecular Deformation in Regenerated Cellulose Fibers. *Biomacromolecules* **2005,** *6*, 507-513.
40. Kroonbatenburg, L. M. J.; Kroon, J.; Northolt, M. G., Chain Modulus and Intramolecular Hydrogen-Bonding in Native and Regenerated Cellulose Fibers. *Polym. Commun.* **1986,** *27*, 290-292.
41. Simon, J. P.; Eriksson, K. E. L., The Significance of Intra-Molecular Hydrogen Bonding in the Beta-O-4 Linkage of Lignin. *J. Mol. Struct.* **1996,** *384*, 1-7.
42. Beste, A.; Buchanan, A. C., III, Kinetic Analysis of the Phenyl-Shift Reaction in Beta-O-4 Lignin Model Compounds: A Computational Study. *J. Org. Chem.* **2011,** *76*, 2195-2203.
43. Beste, A.; Buchanan, A. C., III, Role of Carbon-Carbon Phenyl Migration in the Pyrolysis Mechanism of Beta-O-4 Lignin Model Compounds: Phenethyl Phenyl Ether and Alpha-Hydroxy Phenethyl Phenyl Ether. *J. Phys. Chem. A* **2012,** *116*, 12242-12248.
44. Janesko, B. G., Modeling Interactions between Lignocellulose and Ionic Liquids Using Dft-D. *Phys. Chem. Chem. Phys.* **2011,** *13*, 11393-11401.
45. Janesko, B. G., Acid-Catalyzed Hydrolysis of Lignin Beta-O-4 Linkages in Ionic Liquid Solvents: A Computational Mechanistic Study. *Phys. Chem. Chem. Phys.* **2014,** *16*, 5423-5433.
46. Beste, A.; Buchanan, A. C., III; Harrison, R. J., Computational Prediction of Alpha/Beta Selectivities in the Pyrolysis of Oxygen-Substituted Phenethyl Phenyl Ethers. *J. Phys. Chem. A* **2008,** *112*, 4982-4988.
47. Beste, A.; Buchanan, A. C., III, Computational Study of Bond Dissociation Enthalpies for Lignin Model Compounds. Substituent Effects in Phenethyl Phenyl Ethers. *J. Org. Chem.* **2009,** *74*, 2837-2841.
48. Younker, J. M.; Beste, A.; Buchanan, A. C., III, Computational Study of Bond Dissociation Enthalpies for Substituted Ss-O-4 Lignin Model Compounds. *ChemPhysChem* **2011,** *12*, 3556-3565.
49. Beste, A.; Buchanan, A. C., III, Kinetic Simulation of the Thermal Degradation of Phenethyl Phenyl Ether, a Model Compound for the Beta-O-4 Linkage in Lignin. *Chem. Phys. Lett.* **2012,** *550*, 19-24.
50. Beste, A.; Buchanan, A. C., III, Computational Investigation of the Pyrolysis Product Selectivity for Alpha-Hydroxy Phenethyl Phenyl Ether and Phenethyl Phenyl Ether: Analysis of Substituent Effects and Reactant Conformer Selection. *J. Phys. Chem. A* **2013,** *117*, 3235-3242.
51. Beste, A., Reaxff Study of the Oxidation of Lignin Model Compounds for the Most Common Linkages in Softwood in View of Carbon Fiber Production. *J. Phys. Chem. A* **2014,** *118*, 803-814.
52. Gardrat, C.; Ruggiero, R.; Rayez, M.-T.; Rayez, J.-C.; Castellan, A., Experimental and Theoretical Studies of the Thermal Degradation of a Phenolic Dibenzodioxocin Lignin Model. *Wood Sci. Technol.* **2013,** *47*, 27-41.

53. Mayes, H. B.; Broadbelt, L. J., Unraveling the Reactions That Unravel Cellulose. *J. Phys. Chem. A* **2012,** *116*, 7098-7106.
54. Davis, D. A.; Hamilton, A.; Yang, J.; Cremar, L. D.; Van Gough, D.; Potisek, S. L.; Ong, M. T.; Braun, P. V.; Martinez, T. J.; White, S. R., et al., Force-Induced Activation of Covalent Bonds in Mechanoresponsive Polymeric Materials. *Nature* **2009,** *459*, 68-72.
55. Ong, M. T.; Leiding, J.; Tao, H.; Virshup, A. M.; Martinez, T. J., First Principles Dynamics and Minimum Energy Pathways for Mechanochemical Ring Opening of Cyclobutene. *J. Am. Chem. Soc.* **2009,** *131*, 6377-6379.
56. Kryger, M. J.; Ong, M. T.; Odom, S. A.; Sottos, N. R.; White, S. R.; Martinez, T. J.; Moore, J. S., Masked Cyanoacrylates Unveiled by Mechanical Force. *J. Am. Chem. Soc.* **2010,** *132*, 4558-4559.
57. Lenhardt, J. M.; Ong, M. T.; Choe, R.; Evenhuis, C. R.; Martinez, T. J.; Craig, S. L., Trapping a Diradical Transition State by Mechanochemical Polymer Extension. *Science* **2010,** *329*, 1057-1060.
58. Lenhardt, J. M.; Ogle, J. W.; Ong, M. T.; Choe, R.; Martinez, T. J.; Craig, S. L., Reactive Cross-Talk between Adjacent Tension-Trapped Transition States. *J. Am. Chem. Soc.* **2011,** *133*, 3222-3225.
59. Diesendruck, C. E.; Peterson, G. I.; Kulik, H. J.; Kaitz, J. A.; Mar, B. D.; May, P. A.; White, S. R.; Martínez, T. J.; Boydston, A. J.; Moore, J. S., Mechanically Triggered Heterolytic Unzipping of a Low-Ceiling-Temperature Polymer. *Nature Chem.* **2014,** *6*, 623-628.
60. Wang, J.; Kouznetsova, T. B.; Kean, Z. S.; Fan, L.; Mar, B. D.; Martínez, T. J.; Craig, S. L., A Remote Stereochemical Lever Arm Effect in Polymer Mechanochemistry. *J. Am. Chem. Soc.* **2014,** *136*, 15162-15165.
61. Beste, A., Reaxff Study of the Oxidation of Softwood Lignin in View of Carbon Fiber Production. *Energy Fuels* **2014,** *28*, 7007-7013.
62. Zhang, L.; Gellerstedt, G., NMR Observation of a New Lignin Structure, a Spiro-Dienone. *Chem. Commun. (Cambridge, U. K.)* **2001**, 2744-2745.
63. Zhang, L.; Gellerstedt, G.; Ralph, J.; Lu, F., NMR Studies on the Occurrence of Spirodienone Structures in Lignins. *J. Wood Chem. Technol.* **2006,** *26*, 65-79.
64. Rohrdanz, M. A.; Martins, K. M.; Herbert, J. M., A Long-Range-Corrected Density Functional That Performs Well for Both Ground-State Properties and Time-Dependent Density Functional Theory Excitation Energies, Including Charge-Transfer Excited States. *J. Chem. Phys.* **2009,** *130*, 054112.
65. Wang, L.-P.; Titov, A.; McGibbon, R.; Liu, F.; Pande, V. S.; Martínez, T. J., Discovering Chemistry with an Ab Initio Nanoreactor. *Nature Chem.* **2014,** *6*, 1044-1048.
66. Ufimtsev, I. S.; Martínez, T. J., Quantum Chemistry on Graphical Processing Units. 1. Strategies for Two-Electron Integral Evaluation. *J. Chem. Theory Comput.* **2008,** *4*, 222-231.
67. Ufimtsev, I. S.; Martínez, T. J., Quantum Chemistry on Graphical Processing Units. 3. Analytical Energy Gradients, Geometry Optimization, and First Principles Molecular Dynamics. *J. Chem. Theory Comput.* **2009,** *5*, 2619-2628.
68. Ufimtsev, I. S.; Martinez, T. J., Quantum Chemistry on Graphical Processing Units. 2. Direct Self-Consistent-Field Implementation. *J. Chem. Theory Comput.* **2009,** *5*, 1004-1015.
69. Isborn, C. M.; Luehr, N.; Ufimtsev, I. S.; Martinez, T. J., Excited-State Electronic Structure with Configuration Interaction Singles and Tamm-Dancoff Time-Dependent Density Functional Theory on Graphical Processing Units. *J. Chem. Theory Comput.* **2011,** *7*, 1814-1823.

70. Ufimtsev, I. S.; Luehr, N.; Martinez, T. J., Charge Transfer and Polarization in Solvated Proteins from Ab Initio Molecular Dynamics. *J. Phys. Chem. Lett.* **2011,** *2*, 1789-1793.
71. Kulik, H. J.; Luehr, N.; Ufimtsev, I. S.; Martinez, T. J., Ab Initio Quantum Chemistry for Protein Structures. *J. Phys. Chem. B* **2012,** *116*, 12501-12509.
72. Petachem., http://www.petachem.com.
73. Uhe, A.; Kozuch, S.; Shaik, S., Automatic Analysis of Computed Catalytic Cycles. *J. Comput. Chem.* **2011,** *32*, 978-985.
74. Kozuch, S.; Shaik, S., How to Conceptualize Catalytic Cycles? The Energetic Span Model. *Acc. Chem. Res.* **2011,** *44*, 101-110.
75. Chorkendorff, I.; Niemantsverdriet, J. W., *Concepts of Modern Catalysis and Kinetics*. John Wiley & Sons: 2006.
76. Henderson, T. M.; Izmaylov, A. F.; Scalmani, G.; Scuseria, G. E., Can Short-Range Hybrids Describe Long-Range-Dependent Properties? *J. Chem. Phys.* **2009,** *131*, 044108.
77. Saunders, V. R.; Hillier, I. H., Level-Shifting Method for Converging Closed Shell Hartree-Fock Wave-Functions. *Int. J. Quantum Chem.* **1973,** *7*, 699-705.
78. Liu, F.; Luehr, N.; Kulik, H. J.; Martinez, T. J., Quantum Chemistry for Solvated Molecules on Graphical Processing Units (GPUs) Using Polarizable Continuum Models. **(submitted 2015).**
79. Lange, A. W.; Herbert, J. M., A Smooth, Nonsingular, and Faithful Discretization Scheme for Polarizable Continuum Models: The Switching/Gaussian Approach. *J. Chem. Phys.* **2010,** *133*, 244111.
80. Lange, A. W.; Herbert, J. M., The Polarizable Continuum Model for Molecular Electrostatics: Basic Theory, Recent Advances, and Future Challenges. In *Many-Body Effects and Electrostatics in Multi-Scale Computations of Biomolecules*, Q. Cui, P. R., and M. Meuwly, Ed. 2014.
81. NBO6.0., E. D. Glendening, J, K. Badenhoop, A. E. Reed, J. E. Carpenter, J. A. Bohmann, C. M. Morales, C. R. Landis, and F. Weinhold, Theoretical Chemistry Institute, University of Wisconsin, Madison. 2013.
82. Yuan, T. Q.; Xu, F.; Sun, R. C., Role of Lignin in a Biorefinery: Separation Characterization and Valorization. *J. Chem. Technol. Biotechnol.* **2013,** *88*, 346-352.
83. Davin, L. B.; Lewis, N. G., Lignin Primary Structures and Dirigent Sites. *Curr. Opin. Biotechnol.* **2005,** *16*, 407-415.
84. Kilpeläinen, I.; Tervilä-Wilo, A.; Peräkylä, H.; Matikainen, J.; Brunow, G., Synthesis of Hexameric Lignin Model Compounds. *Holzforschung* **1994,** *48*, 381-386.
85. Kleine, T.; Buendia, J.; Bolm, C., Mechanochemical Degradation of Lignin and Wood by Solvent-Free Grinding in a Reactive Medium. *Green Chem.* **2013,** *15*, 160-166.